İSTANBUL UNIVERSITY CERRAHPAŞA

ORIGINAL ARTICLE
Electrica 2024; 24(1): 140-153

Optimal Design of Fractional Order Tilt-Integral Derivative Controller for Automatic Generation of Power System Integrated with Photovoltaic System

Amiya Kumar Naik, Narendra Kumar Jena, Subhadra Sahoo, Binod Kumar Sahu

Department of Electrical Engineering, Siksha O Anusandhan Deemed to be University, Bhubaneswar, Odisha, India

Cite this article as: A. K. Naik, N. K. Jena, S. Sahoo and B. K. Sahu, "Optimal design of fractional order tilt-integral derivative controller for automatic generation of power system integrated with photovoltaic system," *Electrica*, 24(1), 140-153, 2024.

ABSTRACT

Renewable energy has recently attracted a lot of interest due to its low cost and long-term sustainability. Integration of photovoltaic (PV) system to an existing power system in a large scale is a challenging task. Due to the irregular irradiance, and inertia less system, frequency regulation is a cumbersome task. So, load frequency control is recommended in this article for multi-area power systems that include PV and thermal plant sources. The performance of four competing controllers, namely proportional integral derivative (PID), fractional order PID, tilt-integral-derivative (TID), and fractional order TID (FOTID), is investigated and compared. For obtaining the best performing parameters, honey badger algorithm (HBA) is implemented. Furthermore, the uncertainty is taken into account by varying the system parameters from −20% to 20% in steps of 10%. The suggested competing controllers' performance is evaluated using a dynamic load. Performance of the proposed HBA-based FOTID controller is also studied against a randomly varying load applied in area-1. The work is further extended to a four-area system. Finally, it is observed that HBA-based FOTID controller exhibits superior performance in maintaining the system's frequency and tie-line power when it is subjected to a disturbance.

Index Terms— Automatic generation control, fractional order TID (FOTID) controller, honey badger algorithm, photovoltaic system, TID controller.

Corresponding aswuthor:
Binod Kumar Sahu

E-mail:
binoditer@gmail.com

Received: April 12, 2023

Revision Requested: May 22, 2023

Accepted: August 25, 2023

Publication Date: January 31, 2024

DOI: 10.5152/electrica.2024.23044

I. INTRODUCTION

The goal of a contemporary electric power system (PS) is to offer consumers a safe, dependable, and cost-effective source of electricity. The PS's steady and safe functioning is primarily ensured by maintaining a continual balance between power generation and load demands. There is typically a persistent variation in load demand in real-time operation, which generates a relative balance between load and generation [1]. Renewable energy (RE) has recently attracted a lot of interest around the world due to its low cost and long-term sustainability. The electricity system has become increasingly complex, especially as RE sources (RESs) have become more prevalent. These alternatives are ecologically friendly suppliers that help to reduce the use of fossil fuels and its repercussions in the face of the greenhouse effect. The impact of RESs on load frequency control (LFC) problem studies has been the subject of some critical researches [2].

Due to intermittent or load perturbation, the system frequency oscillates capriciously, which enables an undesired mismatch between generation and demand. This power balance is amended by automatic generation control (AGC) maintaining the frequency to a set value as discussed in [3, 4]. For this, a suitable and well-designed control technique is very much essential.

Classical controllers are used ubiquitously in many industries and in research articles for AGC owing to their simple setup and application. In this regard, some works [5-7] are spelled out using proportional integral derivative (PID) or its variety. Gozde et al. [5] addressed the importance of the secondary controller using Proportional-Integral (PI) and PID controllers for AGC analysis. In [6], a PID controller is equipped in a PS to diminish the oscillation content in the area frequency. To soothe out the harmonic contents in the PID controller, Saikia et al. [8] proposed a double-derivative based PID+DD controller for AGC issue to reap enhanced performance. To augment the control action with independent loops, classical controllers are amended to multiple degrees of freedom (DOFs) and cascaded-based controllers. In this regard, some papers like [9-11] addressed their benefits and analyzed the stability of the system. Along with this, some papers [1, 3, 12, 13]

incited the use of an intelligent controller to tackle the AGC issues effectively. Jyoti et al. [12] designed a type-2 fuzzy controller (FC) to study the AGC of a PS. In this model, a wide operative range of perturbation has been imposed to test the capability of the FC. In the same way, an adaptive FC has been designed by Sahoo et al. [13] to stabilize the interconnected PS so that the power fluctuation ceases to zero. But, in the due course of time, the advent of fractional calculus boosts the potential of PID controller. In this regard, many researchers like [9, 11, 13, 14-20] have focused on fractional order PID (FOPID) controller due to the flexibility in the design process. This salient feature gives a higher possibility of regulating the system dynamics, especially in AGC for enhancing the dynamic responses and system's stability [14-16]. Dating back to 1994, Lurie [17] proposed a tilt-integral derivative (TID) controller and elucidated the advantages over PID controller. In a continuous system domain, the proportional block is replaced with a tilting block denoted by $s^{-1/n}$. It offers the advantages of being easier to tune and having a stronger capacity to reject disturbances. Also, the TID controller is less sensitive to parameter changes that occurred in the system as addressed in [17]. Again, a TID controller in conjunction with a derivative filter known as a TIDF controller was developed and proven to be superior to the PID controller in [18, 19]. In [20], the same fractional order approach is applied to a TID controller, popularly called as FOTID, which is architecturally similar to FOPID, to investigate the performance of AGC in terms of robustness and sensitivity to a wide range of system parameters under various steps and random load disturbances.

For every control system to work optimally, paramount controller tuning is essential to meet the goal. Therefore, many researchers have sought to improve the capabilities of traditional controllers by using a variety of optimization strategies to optimize the gain parameters. In this context, several optimization techniques like selfish herd optimizer [21], genetic algorithm [22], particle swarm optimization [23], artificial bee colony [24, 25], differential evolution [26, 27], and imperialist competitive method in [28, 29] have been endorsed to enumerate the gains optimally so that the system performance is unaltered against wider operating conditions.

Dahiya et al. [30] developed and implemented an optimal global neighborhood algorithm-based PID with filter controller for regulation of frequency in a single-area multi-source PS. Celik et al. [31] proposed a modified salp swarm algorithm for optimally tuning the PID controllers' gains of an AVR system. Hakimuddin et al. [32] presented a study on frequency regulation of a realistic two-area multi-unit PS. Arya [33] implemented an imperialist competition algorithm-based PDF-(1 + PI) controller with capacitive energy storage units to improve the frequency stability of a two-area PS.

The above discussion reveals that the power network comes across intermittent uncertainties, sporadic load changes, nonlinearities, and communication delays. These effects are not suppressed adequately by the classical controllers. Their performance gets subdued under different operating conditions, and in turn response gets sluggish having oscillations. Further, in the case of cascade controllers with different DOF, the control structure becomes more complex, and the slower response of the inner loop causes instability or sluggishness to the system. Similarly, for AGC, fuzzy controllerFCs have gained its popularity but formulating membership functions is an uphill task. It needs an expertise to set the parameters at the input/output. On the other hand, an erroneous selection of fuzzy parameters or membership functions causes horrendous performance. All of the above, if the classical controllers with simple structures are coordinated by fractional/tilted operators, then the modified controller still has great scope to implement in AGC studies. Therefore, in this work, the blend of FOTID controller has been utilized as a secondary controller to improve the system response efficiently. Also, to enumerate the FOTID parameters tightly, the honey badger algorithm (HBA) algorithm has been applied. The major contributions are highlighted below.

The major contribution of this work is as follows:

a. A two-area model comprising a photovoltaic (PV) system and a reheat thermal system is simulated in MATLAB/SIMULINK environment.
b. To enhance the effectiveness of AGC in a PS, various kinds of secondary controllers like PID, TID, FOPID, and FOTID are designed optimally with the help of HBA algorithm.
c. The HBA program is written in a MATLAB .m file, and the two-area SIMULINK model equipped with the proposed controllers is called to optimize the controllers' gains.
d. The performances of the proposed controllers are analyzed by taking various transient parameters such as undershoot/overshoot and settling time.
e. The potential of the HBA algorithm designed FOTID controller over other controllers, published in recent articles, is proved in this study.
f. Robustness of the proposed controller is also verified by randomly varying the load and system parameters.
g. The effectiveness of FOTID controller in comparison to FOPID, TID, and PID controller has been elucidated through a bar chart.
h. Finally, it is seen that the HBA-based FOTID controller exhibits superior performance compared to the others in all aspects.

II. MODELING OF THE POWER SYSTEM

A. Modeling of Photovoltaic System

Extraction of solar energy by PV system is an incredibly intriguing technique. In this sort of RE harvest, different kinds of diversified cutting edge technologies are employed, and its sophisticated

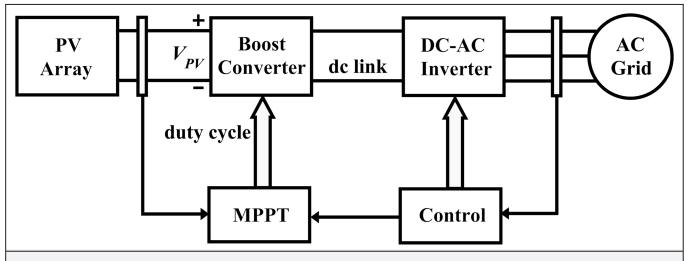

Fig. 1. Photovoltaic system block diagram.

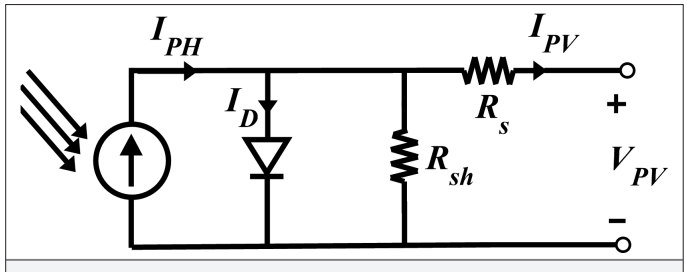

Fig. 2. A solar panel's single diode equivalent circuit.

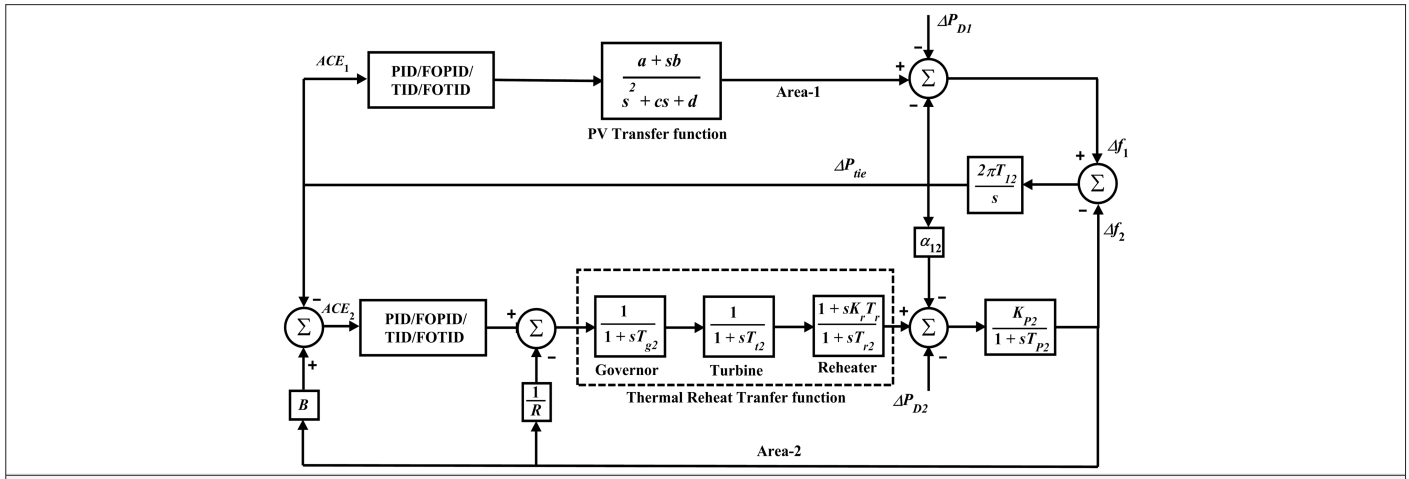

Fig. 3. A test model of a two-area PS [2].

development is going on consistently day by day. Sporadic nature of solar irradiance and temperature, a maximum power point tracking device is employed to extract maximum power by firing the boost converter circuit properly as shown in Fig. 1. Again, the dc output at dc-link is converted to ac which is fed to the grid as shown in Fig. 1. Here, the dc/ac converter supplies the ac power to grid with a suitable voltage and grid frequency.

In this study, a single diode model is taken as illustrated in Fig. 2. The modeling of this solar cell is described as follows.

$$I_{PV} = I_{PH} - I_{D.} - \frac{V_{PV} - I_{PV}.R_{se}}{R_{sh.}} \tag{1}$$

$$I_D = I_o\left[\exp\left(\frac{q_e(V_D - I_{PV}R_{se})}{Ak_bT}\right) - 1\right] \tag{2}$$

$$I_{PH} = \frac{\Psi_{solar}}{1000}\left(I_{SC} + k_1(T - 25)\right) \tag{3}$$

where I_{PV} and V_{PV} are the current and voltage of the PV cell, respectively. Other parameters are I_o = dark saturation current, I_{PH} = photo current, I_D = diode current, V_D = diode voltage, Ψ_{solar} = irradiance, R_{se}/R_{sh} = series/shunt resistance, R_{sh} = shunt resistance, k_b = Boltzmann constant, I_{sc} = short circuit current, q_e = charge of an electron, A = quality factor of a diode, and T = temperature. Converting all the equations of the PV system including converters and filters, the transfer function of the PV system is provided in (4). The simplified model is inherited from the paper [2].

$$G_{PV}(s) = \frac{a + bs}{s^2 + cs + d} \tag{4}$$

The parameters of this transfer function are taken as $a = 900$, $b = 18$, $c = 100$, and $d = 50$ from [2].

B. Modeling of Thermal Power Plant

The governor, turbine, re-heater, and generator make up the thermal generation system in area 2. The following is a list of their transfer functions which are described by (5)–(8). The modeling of each component is taken from [2].

$$G_g(s) = \frac{k_g}{1 + sT_g} \tag{5}$$

$$G_t(s) = \frac{k_t}{1 + sT_t} \tag{6}$$

$$G_r(s) = \frac{1 + sk_rT_r}{1 + sT_p} \tag{7}$$

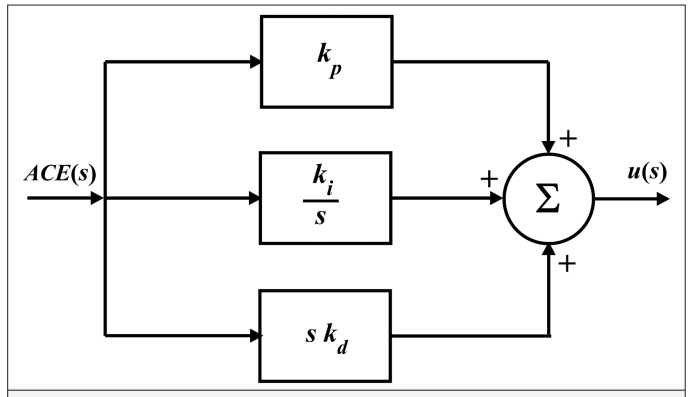

Fig. 4. Control structure of a PID controller.

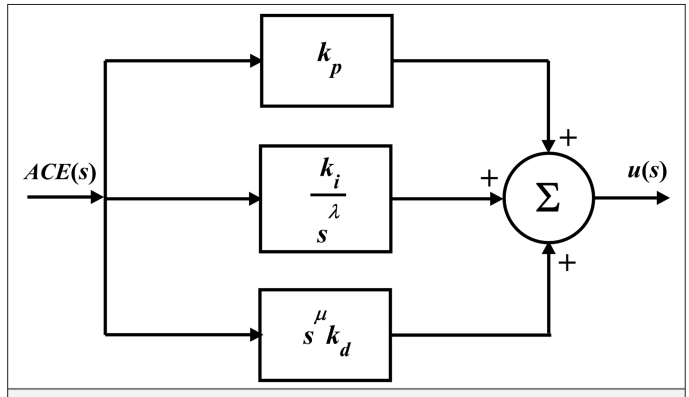

Fig. 5. Control structure of the FOPID controller.

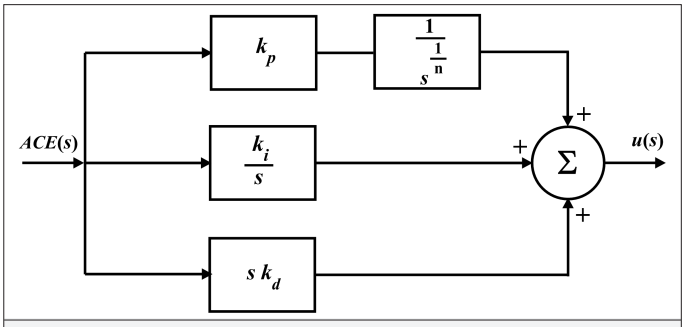

Fig. 6. Control structure of TID controller.

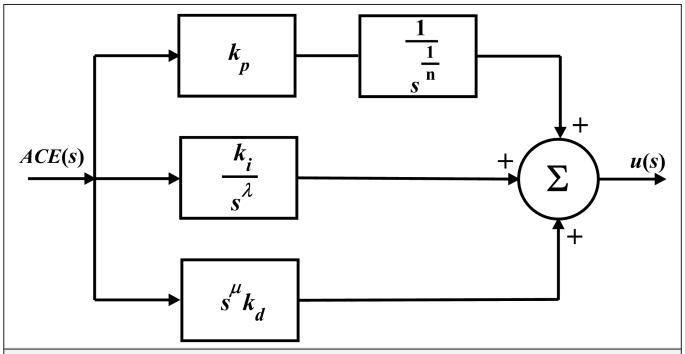

Fig. 7. Control structure of an FOTID controller.

$$G_p(s)=\frac{k_p}{1+sT_p} \tag{8}$$

C. Modeling of Power System

The proposed model is depicted in Fig. 3. Here, in area-1, the PV system is controlled by the proposed PID/TID/FOTID controllers. Similarly, in area-2, the control signal generated by PID/TID/FOTID controllers is passed to the governor of the thermal unit. The load perturbation of ΔP_{D1} and ΔP_{D2} are injected in area-1 and area-2, respectively. The deviations of frequencies (Δf_1 and Δf_2) and tie-line power flow (ΔP_{tie}) are shown in Fig. 3. To minimize the error (deviation of frequency and tie-line power), area control error (ACE) is controlled by processing through the PID/TID/FOTID controllers. The ACE in area-2 is provided in (9), where the dynamics of ΔP_{tie} and Δf are given in (10) and (11), respectively.

$$ACE_2=B_1\Delta f+\Delta P_{tie} \tag{9}$$

$$\Delta P_{tie}=\frac{2*pi*T_{12}}{s}\left(\Delta f_1-\Delta f_2\right) \tag{10}$$

$$\Delta f=\Delta P*\left(\frac{K_P}{1+s.T_P}\right) \tag{11}$$

III. CONTROL METHODOLOGIES

A. Conventional Proportional Integral Derivative Controller

Conventional PID controllers are very popular in process industries because of their simple structure, robustness, and easy-to-understand regulating procedures. They can also provide great control performance despite the process plant's changing dynamic behavior [1]. Fig. 4 illustrates the structure of a PID controller whose transfer function can be expressed as (12).

$$\frac{u(s)}{ACE(s)}=k_p+\frac{k_i}{s}+sk_d \tag{12}$$

wwhere k_p, k_i, and k_d are the proportional, integral, and derivative gain parameters of the PID controller, respectively.

B. Functional Order Proportional Integral Derivative Controller Structure

The FOPID controller, also known as the $PI^{\lambda}D^{\mu}$ controller, is an extension of the ordinary PID controller with a real-order integrator (λ) and a real-order differentiator (μ) whose structure is shown in Fig. 5. In the Laplace domain, the transfer function of this sort of controller is expressed as in (13).

$$\frac{u(s)}{ACE(s)}=k_p+\frac{k_i}{s^{\lambda}}+s^{\mu}k_d \tag{13}$$

TABLE I. DESCRIPTION OF BENCHMARK FUNCTIONS TAKEN IN THE STUDY

Functions	Function's Expression	Dimension	Range
Six-hump camel (F_1)	$f(x)=\left(4-2.1x^2+\frac{x_1^4}{3}\right)x_1^2+x_1x_2+\left(-4+4x_2^2\right)x_2^2$	2	[−3, 3] [−2, 2]
Cross-in-tray (F_2)	$f(x)=-0.0001\left(\left\lvert\sin(x_1)\sin(x_2)\exp\left(\left\lvert 100-\frac{\sqrt{x_1^2+x_2^2}}{\pi}\right\rvert\right)\right\rvert+1\right)^{0.1}$	2	[−10, 10]
Easom (F_3)	$f(x)=-\cos(x_1)\cos(x_2)\exp\left(-(x_1-\pi)^2-(x_2-\pi)^2\right)$	2	[−100, 100]
Hartmann-3D (F_3)	$f(x)=-\sum_{i=1}^{4}\alpha_i exp\left(-\sum_{j=}^{3}A_{ij}\left(x_j-P_{ij}\right)^2\right)$	3	[0, 1]

TABLE II. PERFORMANCE ANALYSIS OF AOA AND IAOA ALGORITHMS

Algorithm	Function	Optimum Value	Minimum	Maximum	Mean	Standard Deviation	Computational Time (s)
HBA	F_1	−1.0316	−1.0316	−1.0316	−1.0316	4.5168×10^{-16}	1.136
DE			−1.0316	−1.0316	−1.0316	1.3437×10^{-15}	1.1209
PSO			−1.0316	−1.0316	−1.0316	8.2866×10^{-12}	1.0381
HBA	F_2	−2.06261	−2.06261	−2.06261	−2.06261	9.2199×10^{-16}	1.6893
DE			−2.06261	−2.06261	−2.06261	2.3930×10^{-11}	1.4469
PSO			−2.06261	−2.06261	−2.06261	3.7111×10^{-9}	1.3765
HBA	F_3	−1	−1	−1	−1	0	0.9664
DE			−1	−1	−1	0	0.8339
PSO			−1	−1	−1	5.8275×10^{-16}	0.6973
HBA	F_4	−3.86278	−3.86278	−3.86278	−3.86278	3.1618×10^{-15}	1.6265
DE			−3.86278	−3.86278	−3.86278	9.7199×10^{-15}	1.2970
PSO			−3.86278	−3.86278	−3.86278	2.9794×10^{11}	1.1493

DE, differential evolution; HBA, honey badger algorithm; PSO, particle swarm optimization.

There are two more parameters in the FOPID controller as compared to traditional PID, non-integer integrator and differentiator orders, respectively. These λ and μ can be any real integers greater than zero. These two additional tuning parameters connected with the FOPID controller make it superior by providing more flexibility for system dynamics modification [11].

C. Tilt-Integral-Derivative Controller Structure

Fig. 6 depicts the structure of a TID controller. It has a PID controller-like configuration, with the proportional element tilted due to the $s^{-1/n}$ transfer function. It allows for easier tuning, improved disturbance rejection, and increased sensitivity to changes in system parameters [17].

Equation (14) is the transfer function expression of a TID controller, respectively.

$$\frac{u(s)}{ACE(s)} = \frac{k_p}{\frac{1}{s^n}} + \frac{k_i}{s} + sk_d \tag{14}$$

D. Functional Order Tilt-Integral-Derivative Controller Structure

As shown in Fig. 7, the structure of a fractional order TID (FOTID) controller is similar to that of a FOPID controller [20], with a fractional order or non-integer order integrator and differentiator. The following is the transfer function for this controller given in (15).

$$\frac{u(s)}{ACE(s)} = \frac{k_p}{\frac{1}{s^n}} + \frac{k_i}{s^\lambda} + s^\mu k_d \tag{15}$$

The fractional orders of the integrator and differentiator are λ and μ, respectively, with all other parameters mentioned above.

IV. HONEY BADGER ALGORITHM

Honey badger algorithm was developed by Hasim et al. [34] in 2022 by mathematically modeling the foraging behavior of honey badger. While searching for food, honey badger either smells and digs or follows the path of honeyguide bird. So, the HBA is mathematically modeled with three phases, namely initialization phase, digging phase, and honey phase as described below.

A. Initialization Phase

In this phase, a probable solution matrix of size $[NP \times D]$ is generated randomly within the predefined search space, where "*NP*" is the size of the population and "*D*" is the dimension of the problem. The initial population is generated using (16):

$$x_i = (u_i - l_i) + l_i \times rand(NP, D) \tag{16}$$

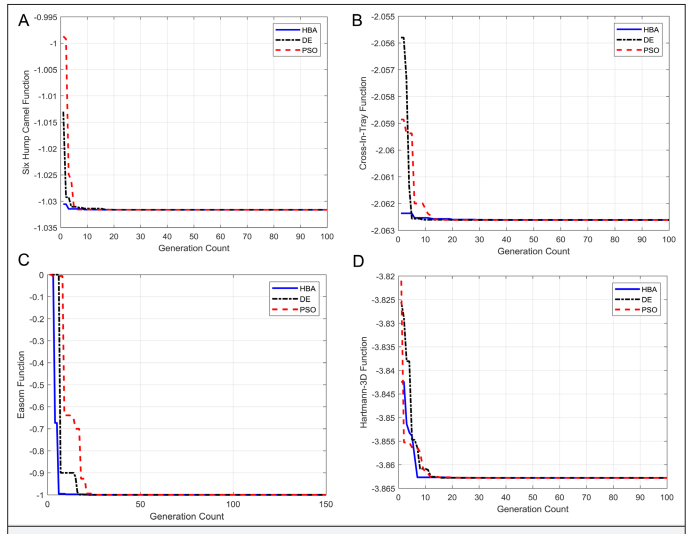

Fig. 8. Convergence characteristics of various benchmark functions: (a) six-hump camel function, (b) cross-IN-tray function, (c) Easom function, an (d) Hartmann-3D function.

TABLE III. OPTIMAL CONTROLLER'S GAINS

PID	K_{p1}	K_{i1}	K_{d1}	K_{p2}	K_{i2}	K_{d2}	ITAE						
	3.4169	3.4956	4.9895	4.9856	4.9153	1.0296	0.3343						
TID	K_{p1}	K_{i1}	K_{d1}	n_1	K_{p1}	K_{i1}	K_{d1}	n_1					
	4.986	2.1718	4.992	4.6237	4.956	1.2057	1.4566	2.82661	0.1986				
FOPID	K_{p1}	K_{i1}	K_{d1}	μ_1	λ_1	K_{p1}	K_{i1}	K_{d1}	μ_1	λ_1			
	4.992	4.998	4.981	0.8225	0.9800	4.972	4.895	2.2867	0.7555	0.9795	0.1586		
FOTID	K_{p1}	K_{i1}	K_{d1}	n_1	μ_1	λ_1	K_{p2}	K_{i2}	K_{d2}	N_2	μ_2	λ_2	
	4.895	**4.998**	**2.076**	**4.991**	**0.0104**	**0.98**	**4.975**	**4.875**	**4.994**	**4.988**	**0.722**	**0.98**	**0.1357**

PID, proportional integral derivative; FOPID, fractional order PID; FOTID, fractional order tilt-integral-derivative; TID, tilt-integral-derivative.
Bold face indicates better results.

where u_i and l_i are the upper and lower limits of the design variables, respectively.

B. Digging Phase

In this phase, the honey badger updates its position by performing digging action similar to the Cardioids' motion which is mathematically modeled as:

$$x_{new} = x_{target} + F \times \beta \times I \times x_{target} + F \times \alpha \times rand \times d_i \times \left|cos(2\pi \times rand) \times \left[1 - cos(2\pi \times rand)\right]\right| \quad (17)$$

where x_{target} is the targeted position of the prey and F is a flag which is helpful in avoiding the local optima by altering the search direction and taken as 1 or -1 as expressed in (16):

$$F = \begin{cases} 1 & if\ rand \le 0.5 \\ -1 & otherwise \end{cases} \quad (18)$$

The variable β indicates the ability to catch food and is taken as 6 in this study; α is the influence factor, which is a time-varying parameter expressed as:

$$\alpha = K \times e^{\left(\frac{-t}{t_{max}}\right)} \quad (19)$$

where K is a constant taken as 2, t is the current iteration, and t_{max} is the maximum number of iterations.

I is the intensity of the smell of the prey, which can be determined by using the inverse square law as given in (20):

$$I_i = \frac{S \times rand}{4\pi d_i^2} \quad (20)$$

where S is the strength of smell concentration of prey and d_i is the distance between the position of badger and prey, which are expressed as:

$$S = \left(x_i - x_{i+1}\right)^2 \quad (21)$$

$$d_i = x_{target} - x_i \quad (22)$$

C. Honey Phase

In this phase, the honey badger follows the path of the honey guide bird to locate the beehive, which can be mathematically expressed as:

$$x_{new} = x_{target} + F \times rand \times \alpha \times d_i \quad (23)$$

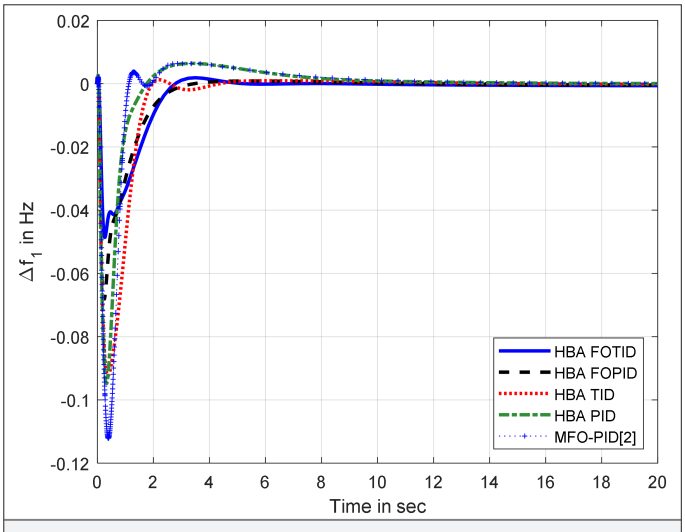

Fig. 9. Frequency deviations in area-1.

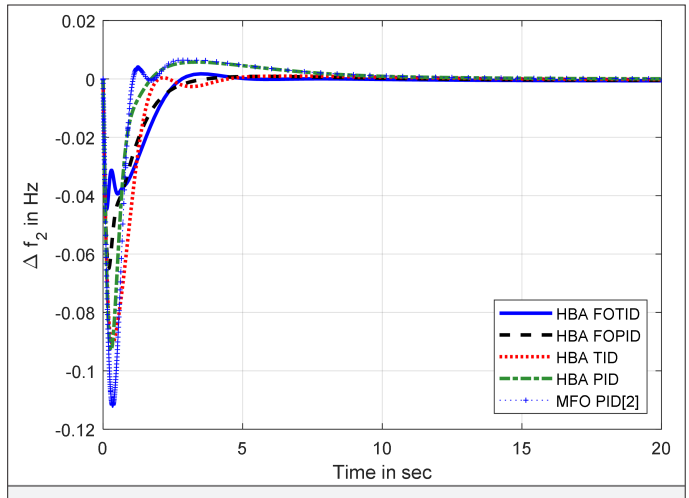

Fig. 10. Frequency deviations in area-2.

TABLE IV. TRANSIENT PERFORMANCE ANALYSIS OF THE PROPOSED POWER SYSTEM WITH DIFFERENT CONTROLLERS

	Δf_1			Δf_2			ΔP_{tie}			
Controller	**Undershoot (×10−³) in Hz**	**Overshoot (×10−³) in Hz**	**Settling time in sec**	**Undershoot (×10−³) in Hz**	**Overshoot (×10−³) in Hz**	**Settling Time in s**	**Undershoot (×10−³) in Hz**	**Overshoot (x10−³) in Hz**	**Settling Time in s**	**ITAE**
GA-PI [2]	−296.39	162.98	18.6449	−243.12	157.37	21.2331	−49.15	57.45	19.8377	12.1241
FA-PI [2]	−315.42	157.88	16.1755	−230.15	124.51	19.2539	−48.33	47.02	21.5314	7.4259
MFO-PI [2]	−112.4	0.33	8.0003	−182.83	42.75	8.9701	−17.47	43.5	10.8708	3.1917
WOA-PI [2]	−202.0	79.67	15.0644	−221.0	99.9	16.0608	−38.81	53.62	15.6427	4.1211
COA-PI [2]	−100.8	0.687	11.8425	−167.8	57.18	12.5183	−19.07	36.91	12.1488	2.682
MFO-PID [2]	−112.83	7.03	7.7267	−111.32	7.12	7.6279	−0.36	3.26	10.8570	0.49854
MWAO-PID [2]	−243.0	9.7233	13.18	−185.6	12.84	10.6333	−2.152	14.59	7.0895	1.4841
HBA-PID	−94.8455	6.4209	4.6964	−92.9565	5.7885	4.4588	−0.6277	1.9495	7.7652	0.3343
HBA-TID	−92.3567	2.7397	1.7018	−90.7081	0.9594	1.6699	−0.8663	1.8950	6.2011	0.1986
HBA-FOPID	−68.3751	2.4669	2.0756	−65.0583	0.8725	2.2191	−0.3989	1.4120	3.5270	0.1586
HBA-FOTID	**−48.5931**	1.8736	2.1962	**−44.6091**	1.7476	2.1962	**−0.2234**	1.9544	**2.9919**	**0.1357**

HBA, honey badger algorithm; PID, proportional integral derivative; FOPID, fractional order PID; FOTID, fractional order tilt-integral-derivative; TID, tilt-integral-derivative.
Bold face indicates better result.

D. Pseudo-code of Honey Badger Algorithm

1) Initialization Phase:

Randomly generate the initial population of size [$NP \times D$] *using (16).*

2) Digging Phase:

Fori=1:NP
Update the position of the honey badger by performing a digging action similar to the Cardioid motion using (17).
end

3) Honey Phase:

Fori = 1: NP
Determine the influence factor (α), intensity of smell (I), strength of smell concentration (S), and distance between the badgers and pray (d) using (19–22), respectively.
Update the position of the particle using (23).
end

Superior performance of the proposed HBA technique against differential evolution (DE) and particle swarm optimization (PSO) is proved by taking four popular benchmark functions. The mathematical

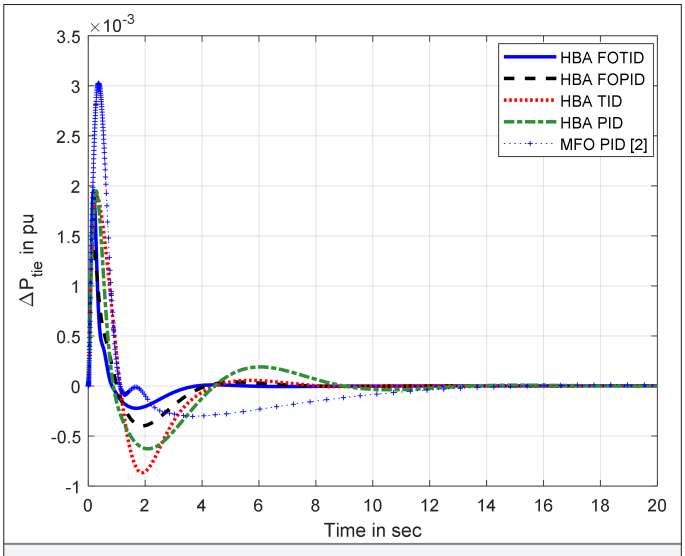

Fig. 11. Tie-line power deviations.

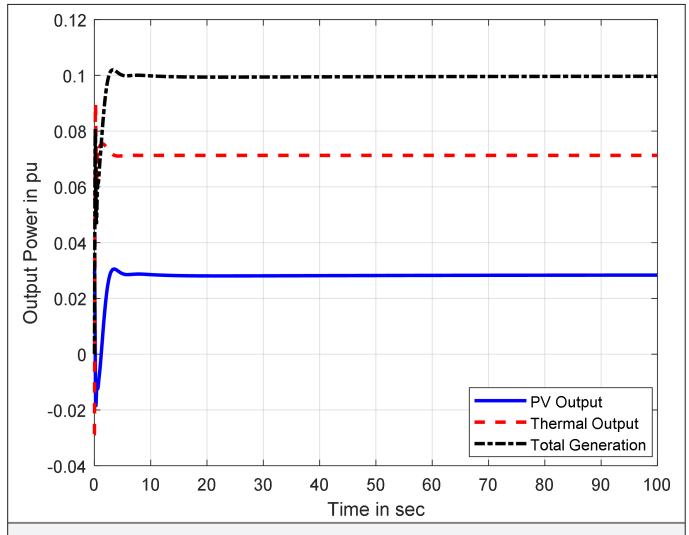

Fig. 12. Output power generation from PV and thermal units.

TABLE V. PERCENTAGE IMPROVEMENTS IN TRANSIENT PERFORMANCE WITH VARIOUS CONTROLLERS AS COMPARED TO THE GA-PI CONTROLLER [2]

	Δf_1			Δf_2			ΔP_{tie}			
Controller	**Undershoot ($\times10^{-3}$) in Hz**	**Overshoot ($\times10^{-3}$) in Hz**	**Settling Time in s**	**Undershoot ($\times10^{-3}$) in Hz**	**Overshoot ($\times10^{-3}$) in Hz**	**Settling Time in s**	**Undershoot ($\times10^{-3}$) in pu**	**Overshoot ($\times10^{-3}$) in pu**	**Settling Time in s**	**ITAE**
FA-PI	−6.4206	3.1292	13.2444	5.3348	20.8807	9.3213	1.6684	18.1549	−8.5378	38.75
MFO-PI	62.0770	99.7975	57.0912	24.7985	72.8347	57.7542	64.4557	24.2820	45.2013	73.67
WOA-PI	31.8466	51.1167	19.2036	9.0984	36.5190	24.3596	21.0376	6.6667	21.1466	66.01
COA-PI	65.9908	99.5785	36.4840	30.9806	63.6652	41.0435	61.2004	35.7528	38.7590	77.88
MFO-PID	61.9319	95.6866	58.5586	54.2119	95.4756	64.0754	99.2675	94.3255	45.2709	95.89
MWAO-PID	18.0134	94.0341	29.3104	23.6591	91.8409	49.9211	95.6216	74.6040	64.2625	87.76
HBA-PID	67.9998	96.0603	74.8113	61.7652	96.3217	79.0007	98.7229	96.6066	60.8563	97.24
HBA-TID	68.8395	98.3190	90.8726	62.6900	99.3904	92.1354	98.2374	96.7015	68.7408	98.36
HBA-FOPID	76.9307	98.4864	88.8677	73.2403	99.4456	89.5489	99.1884	97.5422	82.2207	98.69
HBA-FOTID	**83.6050**	98.8504	88.2209	**81.6514**	98.8895	89.6567	**99.5455**	96.5981	**84.9181**	**98.88**

HBA, honey badger algorithm; PID, proportional integral derivative; FOPID, fractional order PID; FOTID, fractional order tilt-integral-derivative; TID, tilt-integral-derivative.
Bold face indicates better result.

expression, dimension, and search space of the benchmark functions are elaborated in Table I. The statistical performances of HBA, DE, and PSO algorithms are indicated in Table II. The convergence characteristics of the four benchmark functions with HBA, DE, and PSO algorithms are depicted in Fig. 8 (a-d).

From Table II and Fig. 8, it is understood that HBA exhibits better performance compared to DE and PSO algorithms in terms of standard deviation and number of iterations required to converge to the optimum value. But the computation time is greater in HBA because of its complex calculations during exploration and exploitation phases.

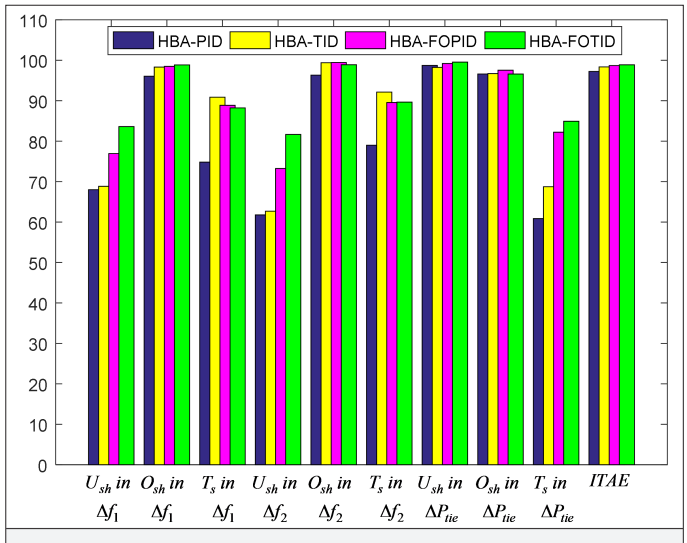

Fig. 13. Bar plot of percentage improvement comparison as compared to the FA-PI controller [2].

With integral of time multiplied absolute error (ITAE), the minimization of error is perceived easily. Here, this cost function is utilized to enumerate the control parameters, and its expression for this proposed model is provided in (24).

$$J_{ITAE\_cost} = \int_0^{t_{sim}} \left[\left(|\Delta f_1| + |\Delta f_2| + |\Delta P_{tie}| \right) * t \right] dt \tag{24}$$

The simulation time is denoted by t_{sim}, along with all of the other parameters described previously. The variables to be optimized in this optimization issue have a lower and an upper limit. Here, the optimization is applied to minimize the deviations of the frequency

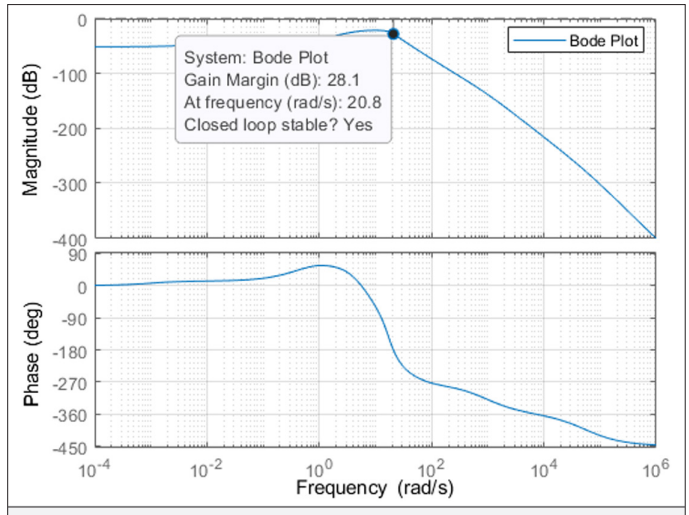

Fig. 14. Bode plot indicating the stability of the system.

TABLE VI TRANSIENT PERFORMANCE ANALYSIS WITH PARAMETER VARIATIONS

		Δf_1			Δf_2			ΔP_{tie}		
Parameters	**% Variation**	**Undershoot ($\times10^{-3}$) in Hz**	**Overshoot ($\times10^{-3}$) in Hz**	**Settling Time in s**	**Undershoot ($\times10^{-3}$) in Hz**	**Overshoot ($\times10^{-3}$) in Hz**	**Settling Time in s**	**Undershoot ($\times10^{-3}$) in pu**	**Overshoot ($\times10^{-3}$) in pu**	**Settling Time in s**
a	−20%	−47.1943	1.8866	2.2464	−44.5527	1.7475	2.2464	−0.2792	2.2678	3.0670
	−10%	−47.9779	1.8771	2.2186	−44.5814	1.7476	2.2186	−0.2484	2.0956	3.0393
	+10%	−49.2207	1.8451	2.2004	−44.6360	1.7415	2.2004	−0.2028	1.8244	3.0501
	+20%	−49.6515	1.8364	2.2029	−44.6619	1.7404	2.2029	−0.1856	1.7151	2.9065
b	−20%	−47.6582	1.8625	2.2205	−44.6413	1.7445	2.2205	−0.2233	1.9082	3.0352
	−10%	−47.9779	1.8771	2.2186	−44.5814	1.7476	2.2186	−0.2484	2.0956	3.0393
	+10%	−49.1051	1.8726	2.1834	−44.5924	1.7439	2.1834	−0.2234	1.9784	3.0350
	+20%	−49.6417	1.8736	2.1820	−44.5751	1.7482	2.1820	−0.2234	2.0029	2.9906
c	−20%	−51.4921	1.8226	2.1168	−44.6252	1.7287	2.1168	−0.1603	1.7489	3.0224
	−10%	−49.9471	1.8476	2.1745	−44.6166	1.7408	2.1745	−0.1908	1.8506	3.0226
	+10%	−47.5424	1.8701	2.2484	−44.6025	1.7493	2.2484	−0.2545	2.0445	3.0756
	+20%	−46.5792	1.9122	2.2754	−44.5967	1.7461	2.2754	−0.2880	2.1352	2.9473
d	−20%	−48.9327	1.8874	2.1901	−44.6092	1.7600	2.1901	−0.2423	1.9503	2.9901
	−10%	−48.7598	1.8806	2.1941	−44.6092	1.7537	2.1941	−0.2328	1.9524	2.9903
	+10%	−48.4328	1.8664	2.1984	−44.6091	1.7412	2.1984	−0.2141	1.9565	2.9935
	+20%	−48.2734	1.8583	2.1929	−44.6090	1.7350	2.1929	−0.2046	1.9585	3.0007
B	−20%	−58.3726	2.3235	2.2422	−50.9454	2.1844	2.2422	−0.2719	2.2543	3.0980
	−10%	−53.0596	2.0779	2.1307	−47.4538	1.9299	2.3366	−0.2438	2.0930	3.0281
	+10%	−44.9187	1.6836	2.0916	−42.1779	1.5524	2.0916	−0.2036	1.8312	2.9517
	+20%	−41.7159	1.5554	2.1632	−40.0924	1.4471	2.1632	−0.1891	1.7237	2.7878
R	−20%	−48.5170	1.6138	2.1886	−44.5763	1.4953	2.1886	−0.2192	1.9525	3.0457
	−10%	−48.5592	1.7559	2.1927	−44.5945	1.6335	2.1927	−0.2215	1.9535	3.0486
	+10%	−48.6209	1.9501	2.1920	−44.6211	1.8345	2.1920	−0.2250	1.9551	3.0577
	+20%	−48.6474	2.0455	2.1962	−44.6311	1.9185	2.1962	−0.2263	1.9557	3.0139
Standard deviation		2.9315	0.1483	0.0411	1.7982	0.1425	0.0481	0.0306	0.1452	0.0641
Mean values		−48.7833	1.8701	2.1942	−44.6997	1.7463	2.2028	−0.2259	1.9668	3.0099
Nominal values		**−48.5931**	1.8736	2.1962	**−44.6091**	1.7476	2.1962	**−0.2234**	1.9544	**2.9919**
Percentage deviation of mean values from nominal values		−0.3914	0.1868	0.0911	−0.2031	0.0744	−0.3005	−1.1191	−0.6345	−0.6016

Bold face indicates nominal values.

and tie-line power flow with the help of J_{ITAE_cost} function. However, the minimizing of the system responses labeled as Δf_1, Δf_2, and ΔP_{tie} is the sole criterion for this performance measure connected to controller parameter optimization. This can be seen in the expression shown in (24). The embedded controllers play an active role in achieving the stated purpose by boosting the dynamic features against the external disturbances as shown in Fig. 3 illustrating the PS model. Peak overshoots and undershoots have been reduced as have the settling durations associated with Δf_1, Δf_2, and ΔP_{tie}. The tweaking of the controller parameters is done using the so-called honey badger algorithm during this procedure. As a result, the following constraints are imposed on the mandated FOTID controller architecture.

$$k_p^{min} \le k_p \le k_p^{max}, k_i^{min} \le k_i \le k_i^{max}, k_d^{min} \le k_d \le k_d^{max},$$

$$n^{min} \le n \le n^{max}, \lambda^{min} \le \lambda \le \lambda^{max} \quad \mu^{min} \le \mu \le \mu^{max}$$

where the superscripts "min" and "max" denote the range of set values of the controller gains to be lied. The controller's gains k_p, k_i, and k_d lay in the range of (0, 5). Similarly, n has been given a range of values between 2 and 3. But, the fractional operators λ and μ are set in between 0 and 1. The above-mentioned boundary conditions must be followed during the optimization process, with no exceptions.

V. RESULTS AND DISCUSSION

Here, the dynamic model (in frequency domain) of the proposed system is deployed in MATLAB/SIMULINK. In this model, an FOTID controller is endorsed to meet the LFC efficiently. To corroborate this, an HBA algorithm is taken to enumerate the gains of the FOTID controller incorporating the ITAE cost function. The dynamic response of the RE integrated system is performed by injecting a load perturbation of 10% pu MW in area-2 at time $t = 0$ s. To advocate its staunch performance, its response is compared with PID, TID, and FOPID controllers. The gains of these controllers are tabulated in Table III.

The dynamic response of frequency in two areas is presented in Figs. 9 and 10. Fig. 11 represents the tie-line power deviation. Here,

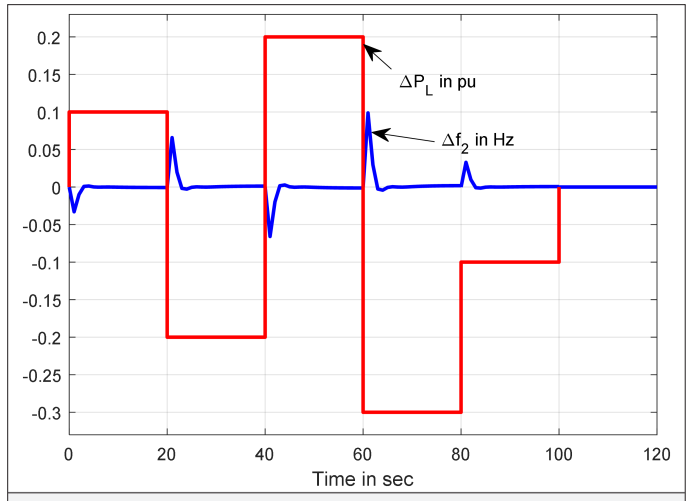

Fig. 16. Randomly applied load in area-1 and the corresponding frequency deviation in area-2.

TID controller expedites the response as the PID controller does. Again, FOPID controller speeds up the response, curtailing the undershoot adequately, which is much better than the TID controller that produces. Further, the FOTID controller ameliorates the frequency deviations profoundly as compared to what PID, TID, and FOPID controllers produce. Similarly, the tie-line power fluctuation ceases promptly under the influence of fractional order controllers. But, the FOTID controller shows a superior performance over the FOPID controller. The complete performance data are presented in Table IV, which shows that the HBA-FOTID controller has yielded a better dynamic response. The total power generation from PV unit and thermal unit are depicted in Fig. 12.

Again, the HBA-based controller's performance over GA/FA/MFO/WOA/COA-based PI controllers and MFO/MWAO-based PID controllers as reported in a recently published research article [2] has been compared. The comparative study as tabulated in Table IV shows that the HBA-FOTID controller has adequately improved the dynamic response. For clear visualization, the percentage

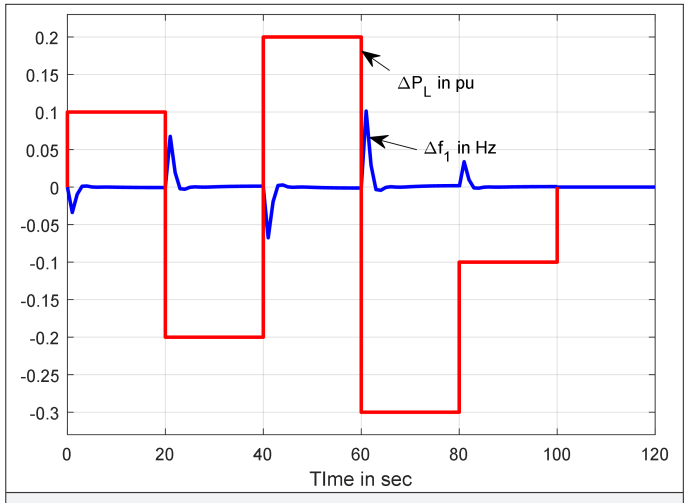

Fig. 15. Randomly applied load in area-1 and the corresponding frequency deviation in area-1.

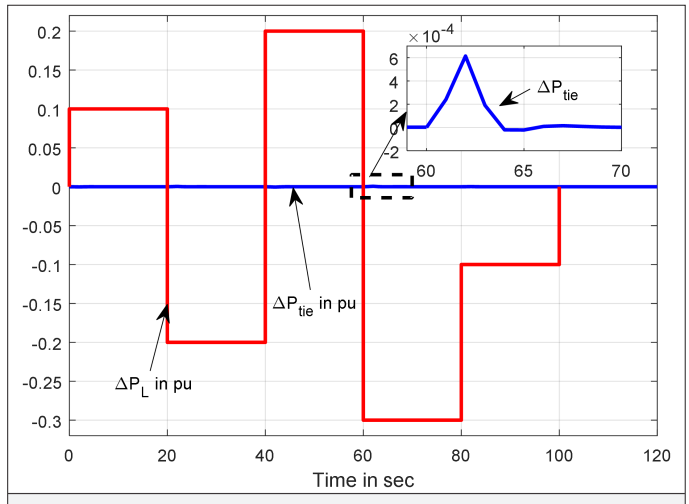

Fig. 17. Randomly applied load in area-1 and the corresponding tie-line power deviation.

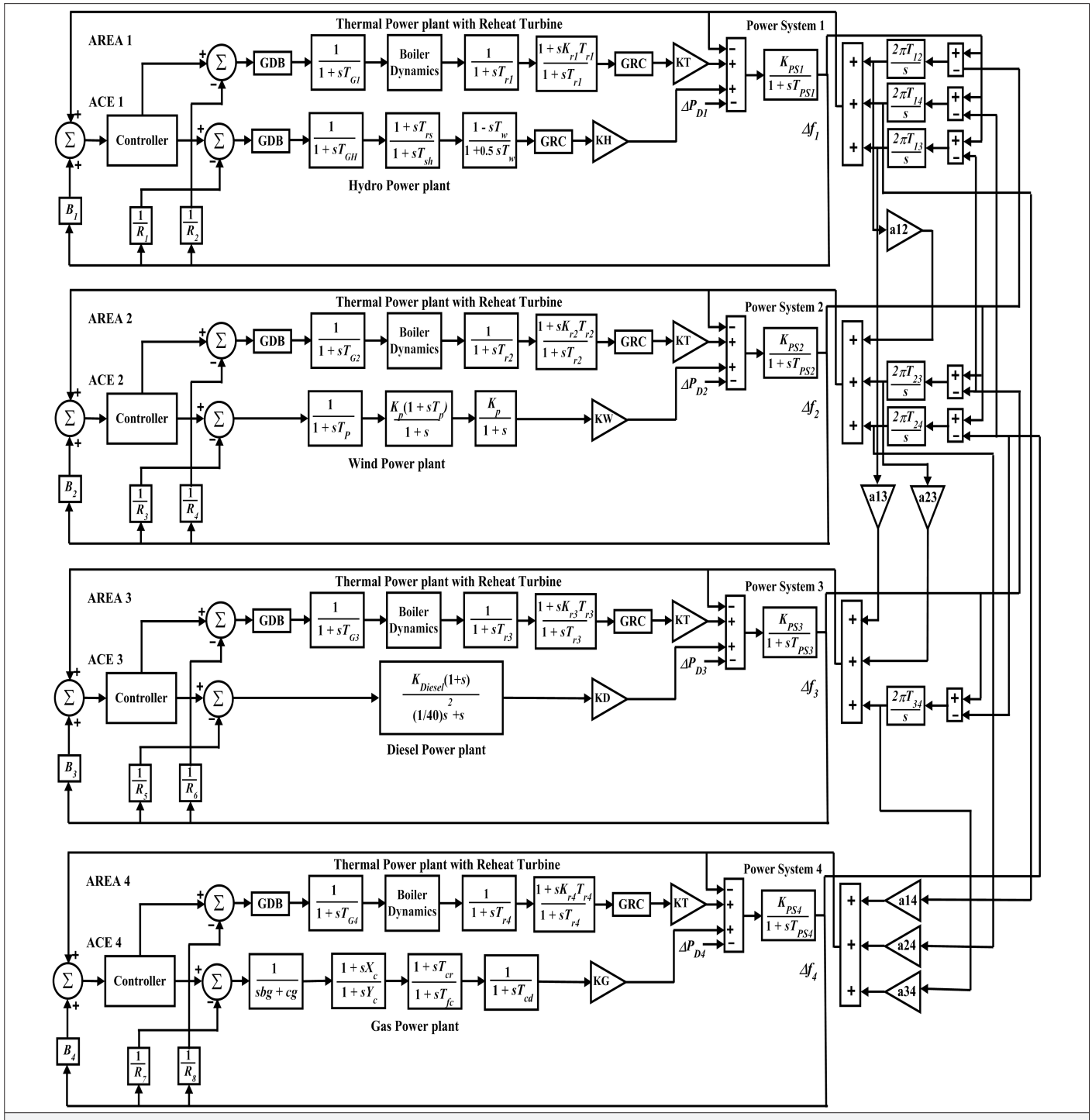

Fig. 18. Transfer function representation of the four-area power system [35].

improvement in various transient parameters with different controllers in comparison with the GA-based PI controller is depicted in Table V. It is seen that the HBA-based FOTID controller is exhibiting a prompt response in comparison to other controllers. Also, the improvement (%) in undershoot/overshoot/settling time of the transient response is presented by a bar chart as given in Fig. 13. Fig. 14 represents the Bode plot of the closed-loop two-area system, which clearly indicates that the system is stable with a 10% disturbance applied in area-2.

A. Robustness Analysis

Robustness of the proposed HBA-based FOTID controller is studied by varying all the system parameters from -20% to +20% in steps of 10%. Transient performance of the PS equipped with HBA-FOTID controller against parametric variations is presented in Table VI. As the standard deviation and percentage deviations of mean values from nominal values of various transient parameters in presented in Table VI are very small, it can be concluded that the proposed HBA-based FOTID controller is robust against parametric variations.

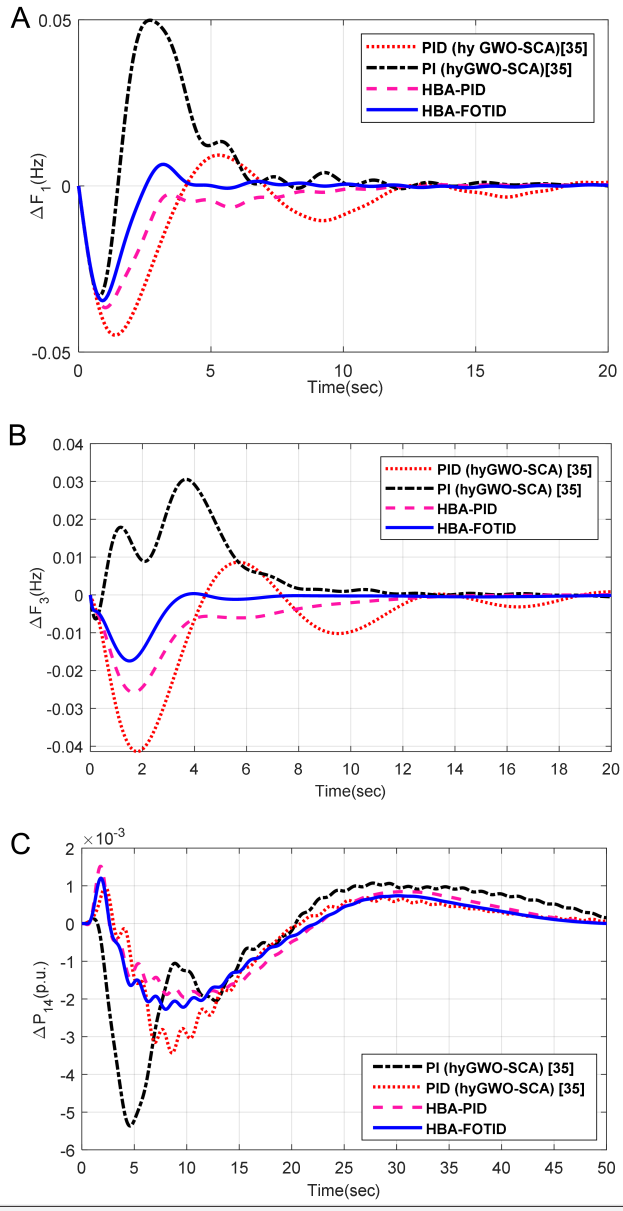

Fig. 19. (a) Frequency deviation in area-1. (b) Frequency deviation in area-2. (c) Tie-line power deviation from area-1 to area-4. (d) Frequency and tie-line power deviations of the four-area system.

Robustness analysis of the proposed FOPID controller is also studied by applying a randomly generated step load in area-1. Frequency deviations in area-1 ānd area-2 and tie-line power deviation along with the random load are shown in Fig. 15, Fig. 16 & Fig. 17 respectively, which clearly indicate the stability of the system even though it is subjected to a disturbance of 0.03 pu. This shows the robustness ability of the proposed controller against random load variations.

B. Extended Work

In order to establish the superiority of the proposed controller (FOTID) and HBA technique, the study is further extended and implemented in a four-area PS, as shown in Fig. 18 [35]. The four-area multi-unit PS consists of thermal-, hydro-, wind-, diesel-, and gas-generating units. Frequency and tie-line power deviations in the four-area PS due to a 2 % sudden change in electrical power demand are depicted in Figs. 19 (a–d). Undershoots and overshoots in the frequency and tie-line power deviations are indicated in Table VII.

From Fig. 19 and Table VII, it is clearly evident that the proposed HBA technique and FOTID controllers show superior dynamic response in comparison with other controllers proposed in [35].

VI. CONCLUSION

An interconnected PS including a renewable source (PV) is modeled, and its simulation for LFC study is performed through Matlab/Simulink platform. Here, the proposed FOTID controller designed by HBA algorithm is producing an ameliorated response in comparison to HBA-PID, HBA-TID, and HBA-FOPID which is expounded from the dynamic response and its specification table. In addition to this, the proposed algorithm-based PID controller has shown an improved response over MFO-PID and MWAO-PID controllers. Again, the deviation of frequency and tie-line power against capricious load change is minimal, which supports the solid design and robust performance of the FOTID controller. Further, the nominal value, mean value, and standard value extend the potential of the designed FOTID controller to implement in a PS for LFC study. To prove the efficacy of the proposed controller, the work is extended to a four-area PS. In the four-area PS, it is seen that the proposed HBA-FOTID controller is showing superior performance. The performance of the test model can be improved by incorporating some non-linear control strategies like sliding mode control, H-infinity control, etc. in the presence of other RE sources incurring intermittent non-linearities.

TABLE VII. TRANSIENT RESPONSE ANALYSIS OF THE FOUR-AREA SYSTEM

	Δf_1			Δf_3			ΔP_{14}		
Controller	**Undershoot ($\times10^{-2}$) in Hz**	**Overshoot ($\times10^{-2}$) in Hz**	**Settling Time in s**	**Undershoot ($\times10^{-2}$) in Hz**	**Overshoot ($\times10^{-2}$) in Hz**	**Settling Time in s**	**Undershoot ($\times10^{-2}$) in Hz**	**Overshoot ($\times10^{-2}$) in Hz**	**Settling Time in s**
PI (hyGWO-SCA) [35]	−3.28	4.88	21.45	−3.28	6.90	20.32	−0.05	0.02	66.74
PID (hyGWO-SCA) [35]	−4.463	1.24	22.92	−4.14	1.20	18.20	−0.32	0.12	50.50
HBA-PID	−3.6635	0.0103	11.82	−2.5787	0.0813	14.63	−0.1956	0.152	43.96
HBA-FOTID	−3.4539	0.0649	8.92	−1.7467	0.0446	7.75	−0.2275	0.1202	41.74

HBA, honey badger algorithm; PID, proportional integral derivative; FOTID, fractional order tilt-integral-derivative.

Peer-review: Externally peer-reviewed.

Author Contributions: Concept – B.K.S., A.K.N.; Design – A.K.N., B.K.S., N.K.J.; Supervision – B.K.S.; Resources –A.K.J., S.S.; Materials – B.K.S., A.K.N., D.S.; Data Collection and/or Processing – A.K.N., N.K.J., S.S., B.K.S.; Analysis and/or Interpretation – B.K.S., N.K.J.; Literature Search – A.K.N., N.K.J., S.S., B.K.S.; Writing – N.K.J., B.K.S.; Critical Review – S.S., B.K.S.

Declaration of Interests: The authors have no conflict of interest to declare.

Funding: The authors declared that this study has received no financial support.

REFERENCES

1. P. K. Mohanty, B. K. Sahu, T. K. Pati, S. Panda, and S. K. Kar, "Design and analysis of fuzzy PID controller with derivative filter for AGC in multi-area interconnected power system," *IET Gener. Transm. Distrib.*, vol. 10, no. 15, pp. 3764–3776, 2016. [CrossRef]
2. A. A. A. El-Ela, R. A. El-Sehiemy, A. M. Shaheen, and A. E. Diab, "Enhanced coyote optimizer-based cascaded load frequency controllers in multi-area power systems with renewable," *Neural Comput. Appl.*, vol. 33, no. 14, pp. 8459–8477, 2021. [CrossRef]
3. N. Nayak, S. Mishra, D. Sharma, and B. K. Sahu, "Application of modified sine cosine algorithm to optimally design PID/fuzzy-PID controllers to deal with AGC issues in deregulated power system," *IET Gener. Transm. Distrib.*, vol. 13, no. 12, pp. 2474–2487, 2019. [CrossRef]
4. K. Ullah,A. Basit,Z. Ullah,S. Aslam,and H. Herodotou, "Automatic generation control strategies in conventional and modern power systems: A comprehensive overview," *Energies*, vol. 14, no. 9, pp. 1–43, 2021. [CrossRef]
5. H. Gozde, M. Cengiz Taplamacioglu, and İ. Kocaarslan, "Comparative performance analysis of artificial bee colony algorithm in automatic generation control for interconnected reheat thermal power system," *Int. J. Electr. Power Energy Syst.*, vol. 42, no. 1, pp. 167–178, 2012. [CrossRef]
6. E. S. Ali, and S. M. Abd-Elazim, "BFOA based design of PID controller for two area load frequency control with nonlinearities," *J. Power Energy Syst.*, vol. 51, pp. 224–231, 2013. [CrossRef]
7. Y. Sharma, and L. C. Saikia, "Automatic generation control of a multiarea ST-thermal power system using grey wolf optimizer algorithm based classical controllers, InternationalJournalofElectrical," *J. Power Energy Syst.*, vol. 73, pp. 853–862, 2015. [CrossRef]
8. L. C. Saikia, and N. Sinha, "Automatic generation control of a multiarea system using ant lion optimizer algorithm based PID plus second order derivative controller, InternationalJournalofElectrical," *J. Power Energy Syst.*, vol. 80, pp. 52–63, 2016. [CrossRef]
9. S. Sahoo, N. K. Jena, P. K. Ray, and B. K. Sahu, "Selfish Herd Optimisation tuned fractional order cascaded controllers for AGC Analysis," *Soft Comput.*, vol. 26, no. 6, pp. 2835–2853, 2022. [CrossRef]
10. R. K. Sahu, S. Panda, U. K. Rout, and D. K. Sahoo, "Teaching learning based optimization algorithm for automatic generation control of power system using 2-dof PID controller," *J. Power Energy Syst.*, vol. 77, pp. 287–301, 2016. [CrossRef]
11. N. K. Jena, S. Sahoo, and B. K. Sahu, "Fractional order cascaded controller for AGC study in power system with PV and diesel generating units," *J. Interdiscip. Math.*, vol. 23, no. 2, pp. 425–434, 2020. [CrossRef]
12. J. R. Nayak, B. Shaw, and B. K. Sahu, "Application of adaptive-SOS (ASOS) algorithm based interval type-2 fuzzy-PID controller with derivative filter for automatic generation control of an interconnected power system," *Eng. Sci. Technol. An Int. J.*, vol. 21, no. 3, pp. 465–485, 2018. [CrossRef]
13. S. Sahoo, N. K. Jena, G. Dei, and B. K. Sahu, "Self-adaptive fuzzy-PID controller for AGC study in deregulated Power System," *Indonesian J. Electr. Eng. Inform.*, vol. 7, no. 4, pp. 650–663, 2019. [CrossRef]
14. R. Matusu, "Application of fractional order calculus to control Theory," *Int. J. Math. Models Methods Appl. Sci.*, vol. 5, no. 7, pp. 1162–1169. Available: https://doi.org/1.05/2.1.00/03.0089, 2011.
15. S. Debbarma, L. C. Saikia, and N. Sinha, "AGC of a multi-area thermal system under deregulated environment using a non-integer controller," *Electr. Power Syst. Res.*, vol. 95, pp. 175–183, 2013. [CrossRef]
16. I. Pan, and S. Das, "Fractional-order load-frequency control of interconnected power systems using chaotic multi-objective optimization," *Appl. Soft Comput.*, vol. 29, pp. 328–344, 2015. [CrossRef]
17. B. J. Lurie, "Three-parameter tunable tilt-integral-derivative (TID) controller", US Patent 5, 1994.
18. R. Kumar Sahu, S. Panda, A. Biswal, and G. T. Chandra Sekhar, "Design and analysis of tilt integral derivative controller with filter for load frequency control of multi-area interconnected power systems," *ISA Trans.*, vol. 61, pp. 251–264, 2016. [CrossRef]
19. R. K. Sahu, G. T. C. Sekhar, and S. Priyadarshani, "Differential evolution algorithm tuned tilt integral derivative controller with filter controller for automatic generation control," *Evol. Intell.*, vol. 14, no. 1, pp. 5–20, 2021. [CrossRef]
20. S. Priyadarshani, K. R. Subhashini, and J. K. Satapathy, "Pathfinder algorithm optimized fractional order tilt-integral-derivative (FOTID) controller for automatic generation control of multi-source power system," *Microsyst. Technol.*, vol. 27, no. 1, pp. 23–35, 2021. [CrossRef]
21. N. K. Jena, S. Sahoo, B. K. Sahu, J. R. Nayak, and K. B. Mohanty, "Fuzzy adaptive selfish herd optimization based optimal sliding mode controller for frequency stability enhancement of a microgrid," *Eng. Sci. Technol. An Int. J.*, vol. 33, p. 101071, 2022. [CrossRef]
22. R. A. Krohling, and J. P. Rey, "Design of optimal disturbance rejection PID controllers using genetic algorithms," *IEEE Trans. Evol. Comput.*, vol. 5, no. 1, p. 78–82, 2001. [CrossRef]
23. Z. L. Gaing, "A particle swarm optimization approach for optimum design of PID controller in AVR system," *IEEE Trans. Energy Convers.*, vol. 19, no. 2, pp. 384–391, 2004. [CrossRef]
24. H. Gozde, and M. C. Taplamacioglu, "Comparative performance analysis of artificial bee colony algorithm for automatic voltage regulator (AVR) system," *J. Franklin Inst.*, vol. 348, no. 8, pp. 1927–1946, 2011. [CrossRef]
25. P. K. Mohanty, B. K. Sahu, and S. Panda, "Tuning and assessment of proportional–integral–derivative controller for an automatic voltage regulator system employing local unimodal sampling algorithm," *Electr. Power Compon. Syst.*, vol. 42, no. 9, pp. 959–969, 2014. [CrossRef]
26. R. K. Sahu, S. Panda, and U. K. Rout, "DE optimized parallel 2-dof PID controller for load frequency control of power system with governor dead-band nonlinearity," *Int. J. Electr. Power Energy Syst.*, vol. 49, pp. 19–33, 2013. [CrossRef]
27. B. Mohanty, S. Panda, and P. K. Hota, "Controller parameters tuning of differential evolution algorithm and its application to load frequency control of multi-source power system," *Int. J. Electr. Power Energy Syst.*, vol. 54, pp. 77–85, 2014. [CrossRef]
28. S. Debbarma, L. C. Saikia, and N. Sinha, "Automatic generation control using two degree of freedom fractional order PID controller," *Int. J. Electr. Power Energy Syst.*, vol. 58, pp. 120–129, 2014. [CrossRef]
29. T. K. Mohapatra, A. K. Dey, and B. K. Sahu, "Employment of quasi oppositional SSA-based two-degree-of-freedom fractional order PID controller for AGC of assorted source of generations," *IET Gener. Transm. Distrib.*, vol. 14, no. 17, pp. 3365–3376, 2020. [CrossRef]
30. P. Dahiya, P. Mukhija, and A. R. Saxena, "Event-triggered based decentralised control for frequency regulation of power systems," *IET Gener. Transm. Distrib.*, vol. 14, no. 10, pp. 2004–2015, 2020. [CrossRef]
31. E. Celik, N. Ozturk, and Y. Arya, "Advancement of the search process of salp swarm algorithm for global optimization problems," *Expert Syst. Appl.*, vol. 182, p.115292, 2021. [CrossRef]
32. N. Hakimuddin, I. Nasiruddin, T. S. Bhatti, and Y. Arya, "Optimal automatic generation control with hydro, thermal, gas, and wind power plants in 2-area interconnected power system," *Electr. Power Compon. Syst.*, vol. 48, no. 6–7, pp. 558–571, 2020. [CrossRef]
33. Y. Arya, "AGC of PV-thermal and hydro-thermal power systems using CES and a new multi-stage FPIDF-(1+ PI) controller," *Renew. Energy*, vol. 134, pp. 796–806, 2019. [CrossRef]
34. F. A. Hashim, E. H. Houssein, K. Hussain, M. S. Mabrouk, W. Al-Atabany, and H. Badger, "Honey Badger Algorithm: New metaheuristic algorithm for solving optimization problems," *Math. Comput. Simul.*, vol. 192, pp. 84–110, 2022. [CrossRef]
35. P. C. Sahu, R. C. Prusty, and S. Panda, "Approaching hybridized GWO-SCA based type-II fuzzy controller in AGC of diverse energy source multi area power system," *J. King Saud Univ. Eng. Sci.*, vol. 32, no. 3, pp. 186–197, 2020. [CrossRef]

Amiya Kumar Naik is currently working as Associate Professor in Department of Electrical Engineering at ITER, Siksha "O" Anusandhan Deemed to be University. He has an industrial experience of near about 7 years in OPTCL and teaching experience is of about 15 years. He completed his graduation from College of Engineering & Technology, Bhubaneswar in the year 1991 and he pursued his Masters from NIT, Rourkela in the year 2011. He has completed his Ph. D. from SOA Deemed to be University in the year 2020. He has more than 24 international publications.

Narendra Kumar Jena received his M. Tech. from the Siksha 'O' Anusandhan (Deemed to be) University, Bhubaneswar in 2013. Presently he is an Assistant professor in ITER, SOA (Deemed to be) University, Bhubaneswar, Odisha, India. He is a member of IEEE since 2014. He has completed his Ph. D. from SOA Deemed to be University in the year 2022. His area of research interest includes Automatic Generation Control, and Renewable energy system stability using Fuzzy logic based Controllers & Robust controllers endorsing Soft Computing Techniques.

Dr. Subhadra Sahoo received B.E. in Electrical Engineering from C.V. Raman College of Engineering, Bhubaneswar, India, in 2006, M. Tech. from C.V. Raman College of Engineering, Bhubaneswar, India, in 2010. She has received her Ph.d degree in electrical engineering from SOA Deemed to be university, Bhubaneswar, Odisha in 2022. Presently she is working as Assistant Professor in ITER, SOA University. Her research interests include Automatic Generation Control, Fuzzy Logic based Controllers, soft computing techniques and renewable energy sources.

Binod Kumar Sahu received his Bachelor's degree in Electrical Engineering from the Institution of Engineers, India, in 2001, his M. Tech. from NIT Warangal in 2003 and Ph. D from Siksha 'O' Anusandhan (Deemed to be) University in 2016. Presently he is working as Professor in ITER, SOA (Deemed to be) University, Bhubaneswar, Odisha, India. He is a member of IET and IEEE since 2014. His area of research interest includes Automatic Generation Control, Fuzzy Logic based Control, Time Series Forecasting and Soft Computing Techniques.